



Epstein-Barr virus-infected plasma cells in periodontitis lesions

Charles V. Olivieri, Hélène Raybaud, Lilit Tonoyan, Sarah Abid, Robert Marsault, Marlène Chevalier, Alain Doglio, Séverine Vincent-Bugnas

► To cite this version:

Charles V. Olivieri, Hélène Raybaud, Lilit Tonoyan, Sarah Abid, Robert Marsault, et al.. Epstein-Barr virus-infected plasma cells in periodontitis lesions. *Microbial Pathogenesis*, 2020, 143, pp.104128 -. [10.1016/j.micpath.2020.104128](https://doi.org/10.1016/j.micpath.2020.104128). <hal-03489843>

HAL Id: hal-03489843

<https://hal.science/hal-03489843v1>

Submitted on 22 Aug 2022

HAL is a multi-disciplinary open access archive for the deposit and dissemination of scientific research documents, whether they are published or not. The documents may come from teaching and research institutions in France or abroad, or from public or private research centers.

L'archive ouverte pluridisciplinaire **HAL**, est destinée au dépôt et à la diffusion de documents scientifiques de niveau recherche, publiés ou non, émanant des établissements d'enseignement et de recherche français ou étrangers, des laboratoires publics ou privés.



Distributed under a Creative Commons CC BY-NC 4.0 - Attribution - Non-commercial use - International License

A STUDY OF CHLOROBENZENE PYROLYSIS

Nicolas Vin¹, Frédérique Battin-Leclerc¹, Hervé Le Gall¹, Nadia Sebbar², Henning Bockhorn²,

Dimosthenis Trimis², Olivier Herbinet^{1*}

¹Laboratoire Réactions et Génie des Procédés, CNRS, Université de Lorraine, BP 20451, 1 rue Grandville, 54000 Nancy, France.

² Combustion Technology, Engler-Bunte-Institute, Karlsruhe Institute of Technology (KIT) Engler-Bunte Ring 7, 76131 Karlsruhe, Germany

* Corresponding author: olivier.herbinet@univ-lorraine.fr

Method of determination: method 1

Colloquium: Gas-Phase Reaction kinetics

Abstract	239	239
Main Text	3403	3681
References	$(25+2) \times (2.3 \text{ lines/reference}) \times (7.6 \text{ words/line})$	472
Figures and captions		
<i>Figure 1</i>	$(137.3\text{mm}+10\text{mm}) \times (2.2 \text{ words/mm}) \times 1 + (57)$	380
<i>Figure 2</i>	$(45.8\text{mm}+10\text{mm}) \times (2.2 \text{ words/mm}) \times 1 + (26)$	146
<i>Figure 3</i>	$(155.3\text{mm}+10\text{mm}) \times (2.2 \text{ words/mm}) \times 1 + (89)$	453
<i>Figure 4</i>	$(87.1\text{mm}+10\text{mm}) \times (2.2 \text{ words/mm}) \times 2 + (79)$	507
<i>Figure 5</i>	$(53\text{mm}+10\text{mm}) \times (2.2 \text{ words/mm}) \times 1 + (29)$	168
Tables		
<i>Table 1</i>	$(5+2\text{lines}) \times (7.6\text{words/line}) \times (2)$	106
<i>Table 2</i>	$(11+2\text{lines}) \times (7.6\text{words/line}) \times (2)$	198
TOTAL (excl. abstract)		6111

Color figures in electronic version only

Supplemental Material is available

A STUDY OF CHLOROBENZENE PYROLYSIS

Nicolas Vin¹, Frédérique Battin-Leclerc¹, Hervé Le Gall¹, Nadia Sebbar², Henning Bockhorn²,

Dimosthenis Trimis², Olivier Herbinet^{1*}

¹Laboratoire Réactions et Génie des Procédés, CNRS, Université de Lorraine, BP 20451, 1 rue
Grandville, 54000 Nancy, France.

² Combustion Technology, Engler-Bunte-Institute, Karlsruhe Institute of Technology (KIT) Engler-
Bunte Ring 7, 76131 Karlsruhe, Germany

Abstract

The pyrolysis of chlorobenzene under dilute atmosphere and quasi-atmospheric pressure was studied at temperatures from 800 to 1150 K using a fused silica jet stirred reactor (JSR) and from 800 to 1250 K in an alumina tubular reactor. Chlorobenzene was chosen as a surrogate to model the thermal decomposition of polychlorinated biphenyls (PCBs). In jet stirred reactor, a maximum chlorobenzene conversion of 48.5 % was observed at a residence time of 2 s, a temperature of 1150 K and an inlet mole fraction of chlorobenzene of 0.005. The following species were quantified: benzene (the major product), HCl, methane, ethylene, acetylene, biphenyl, 1-, 2- and 3-chlorobiphenyl, biphenylene and six isomers of dichlorobiphenyls. In tubular reactor, a maximum chlorobenzene conversion of 95 % was observed at a temperature of 1250 K under the same conditions as in the jet stirred reactor. The same reaction products were detected but with a larger formation of acetylene and methane and a smaller production of chlorinated and bicyclic compounds. The effect of two H-atom donors, methane and hydrogen, has been investigated in JSR. Hydrogen addition has a strong inhibiting effect on the formation of chlorinated and bicyclic products. A new detailed kinetic model was developed and gave a good prediction of the global

reactivity, the formation of most major products, and the effect of the addition of hydrogen and methane. Flow rate and sensitivity analyses have been made to explain the effect of H-atom donors.

Keywords: PCBs, pyrolysis, chlorobenzene, modeling, hydrogen addition.

1. Introduction

Chlorinated compounds are widely used in the chemical industry. The industrial value of the polychlorobiphenyls (PCBs) resulted from their high thermal stability, chemical inertness and non-flammability coupled with excellent electrical properties [1]. The commercial production of PCBs started in 1929 but their use has been banned or severely restricted in many countries since the 70s because of possible risks to human health and environment [1]

Since 1929, around 2 million tons of PCBs have been produced, about 10% of which still remains in the environment today [1]. The sources of PCBs pollution are landfills containing transformers, capacitors and other PCB wastes [1]. While incineration is currently the most widespread disposal technique to treat wastes contaminated by PCBs, it can be a source of dioxins. It is why it is of interest to study an alternative process working in absence of oxygen, such as thermal decomposition. It is crucial then to understand the chemistry of the thermal decomposition of PCBs to predict the influence of operating conditions on the nature and concentration of reaction products. Chlorobenzene was chosen as a surrogate to model the thermal destruction of PCBs.

Because of the large range of temperatures which needs to be investigated, different experimental facilities were previously used to study the thermal decomposition of chlorobenzene: shock tubes [2] [3] [4] [5] to study temperatures above 1500 K and plug flow reactors for lower temperatures [6] [7] [8] [9] [10]. In all those studies, benzene and HCl were the main products of the degradation of chlorobenzene. In terms of products with high molar mass, naphthalene, chloronaphthalene, acenaphthylene, biphenyl and all isomers of chlorobiphenyls and dichlorobiphenyls were found in small amounts [6] [7] [8] [9] [10]. Traces of cyclopentadiene and some substituted benzenes were detected [10]. Some of these studies were performed in presence of a hydrogen donor, generally H₂, which enhances the conversion of C₆H₅Cl into benzene and HCl [2] [10].

The objective of this study is to investigate chlorobenzene pyrolysis using two different types of

reactors: a Jet Stirred Reactor (JSR) and a Tubular Reactor (TR) in order to better understand the chemistry of chlorinated polycyclic compounds. No previous study was performed about the pyrolysis of chlorobenzene in a JSR. A new detailed kinetic model has been developed to reproduce these experimental results.

2. Experimental procedure

Reactants entered the spherical fused silica **jet-stirred-reactor (JSR)**, volume of 85 cm³) through an injection cross made of four nozzles which was located at its center and created high turbulence to produce homogeneity in composition and temperature of the gas phase. The isothermal JSR was preceded by a quartz annular preheating zone in which the temperature of the gas is increased up to the reactor temperature. The gas residence time inside the annular preheater was very short compared to its residence time inside the reactor (a few percent). Both the reactor and the preheating zone were heated by the means of Thermocoax resistances rolled up around the reactor. The reaction temperature was measured by a thermocouple located inside the intra-annular space of the preheating zone; its extremity being placed at the level of the injection cross. Experiments in the JSR were performed at a constant pressure of 106.7 kPa, at a residence time of 2 seconds and at temperatures ranging from 800 to 1150 K. Experimental studies in the **tubular reactor (TR)** have been performed using a horizontal 60 cm long alumina tube (volume of 294 cm³) with an inner diameter of 20 mm and an outer diameter of 25 mm. The ends of the reactor were connected to 2.54 cm (1-inch) diameter Swagelok unions and sealed with high temperature epoxy resin from Final Crotonics. The tubular reactor was heated by an electrical furnace from Vecstar equipped with an S-type thermocouple. For each set reaction temperature, a temperature profile (temperature versus position in the tubular reactor) was measured using a S-type thermocouple (see measured profiles in fig. S1 in Supplementary materials (SM)). Experiments were performed at a constant pressure of 106.7 kPa, at a residence time in the set-point temperature zone

around 2 seconds and at temperatures ranging from 800 to 1300 K. Simulations were performed assuming the TR can be modeled as a plug flow reactor (see discussion in SM) and using the measured temperature profiles.

As shown in Table 1, three reaction mixtures were studied: neat chlorobenzene, addition of hydrogen, and addition of methane.

Table 1: Experimental inlet composition.

Mixture	Neat chlorobenzene	+ H ₂	+CH ₄
Composition (%)	0.5 C ₆ H ₅ Cl + 99.5 He	0.5 C ₆ H ₅ Cl + 0.5 H ₂ + 99.0 He	0.5 C ₆ H ₅ Cl + 0.5 CH ₄ + 99.0 He
Used reactors	JSR and TR	JSR	JSR

Helium, methane and hydrogen were provided by Messer (purity of 99.999 %) and the chlorinated reactant was purchased from Sigma-Aldrich (purity of 99.5%). Gas flow rates were controlled by mass flow controllers and the liquid flow rate by a Coriolis flow controller. The uncertainty in the flow measurements was around 0.5% for each controller, so about 1% on the residence time.

Using a heated transfer line maintained at 433 K to avoid product condensation, the gases leaving the reactors were analyzed using:

- **Gas chromatography (GC):** a first chromatograph, fitted with a PlotQ capillary column, a thermal conductivity detector (TCD) and a flame ionization detector (FID), was used for the quantification of methane, ethylene, acetylene and ethane; a second chromatograph, fitted with a HP-1 capillary column and a FID, was used for the quantification of other types of molecules. The identification of reaction products was performed using a gas chromatograph equipped with a HP-5MS capillary column and coupled to a mass spectrometer. Response factors were determined by injecting calibration mixtures or using the effective carbon number method. Relative uncertainties in mole fractions were estimated to be $\pm 5\%$ for species which were calibrated using standards and $\pm 10\%$ for other ones.

- **A Fourier Transform InfraRed spectrometer (FTIR)** from Thermo Scientific Antaris equipped with a Mercure Cadmium Telluride photoelectric detector. FTIR was used to analyze chlorobenzene and HCl. FTIR calibrations were obtained by injecting standards. A typical FTIR spectrum obtained during chlorobenzene pyrolysis is given in SM.

Notice that, despite high dilution in helium, the experimental results presented hereafter were challenging to obtain. The pyrolysis of chlorobenzene leads at high temperature to the formation of high molecular weight polycyclic aromatic compounds which can condensate in our experimental setup or often plug the injection valves inside our gas chromatographs, leading to large overpressure inside our experimental setup (especially in JSR experiments).

3. Kinetic model

Simulations were performed using the OpenSmoke package [11] and a newly developed detailed chemical kinetic reaction mechanism for chlorobenzene pyrolysis including 224 species in 1455 reactions (given in SM under Chemkin format). Rate parameters were taken from the literature when available. Calculations using quantum methods were carried out when no data were available (See table 2).

Table 2: Theoretically calculated rate constants (rate parameters of reaction 1 have been recalculated in the present study).

	Reaction	A factor ($\text{cm}^3\cdot\text{mol}^{-1}\cdot\text{s}^{-1}$)	n	Ea ($\text{cal}\cdot\text{mol}^{-1}$)
1	$\text{C}_6\text{H}_5 + \text{H}_2 = \text{C}_6\text{H}_6 + \text{H}$	5.02×10^{11}	-0.14	2749
2	$\text{PHICl} + \text{H} = \text{R2PHICl} + \text{H}_2$	1.50×10^8	1.79	12328
3	$\text{PHICl} + \text{H} = \text{R3PHICl} + \text{H}_2$	1.23×10^8	1.81	10930
4	$\text{PHICl} + \text{H} = \text{R4PHICl} + \text{H}_2$	1.35×10^8	1.81	11748
5	$\text{PHICl} + \text{H} = \text{C}_6\text{H}_5 + \text{HCl}$	1.61×10^9	1.57	10988
6	$\text{PHICl} + \text{H} = \text{C}_6\text{H}_6 + \text{Cl}$	4.26×10^7	1.772	7951
7	$\text{PHICl} + \text{Cl} = \text{PHI12Cl}_2 + \text{H}$	1.17×10^4	2.992	22576
8	$\text{PHICl} + \text{Cl} = \text{PHI13Cl}_2 + \text{H}$	8.57×10^3	3.057	21927
9	$\text{PHICl} + \text{Cl} = \text{PHI14Cl}_2 + \text{H}$	5.48×10^3	3.027	21829
10	$\text{PHICl} + \text{H}_2 = \text{C}_6\text{H}_6 + \text{HCl}$	1.36×10^6	2.18	73174

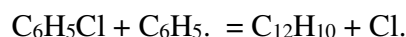
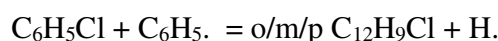
Kinetics parameters of the reaction $C_6H_6 + H = C_6H_5 + H_2$ (Reaction 1) have already been calculated by several authors such like Zhang et al. [12] or Giri et al. [13].

The model is based on that proposed by Husson et al. [14] for the oxidation of ethyl-benzene. The rate constant of reaction 1 in table 2, already presents in the model of Husson [14], has been recalculated.

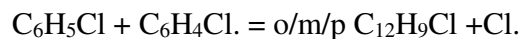
The reactions of the H/Cl system involving HCl, Cl₂, and Cl radicals were taken from Pelucchi et al. [15].

The following types of reactions were added to account for the reactant consumption:

- Unimolecular initiations by breaking a C-H or a C-Cl bond; the C-Cl bond (95 kcal/mol [16]) is the weakest one in the chlorobenzene molecule (C₆H₅Cl, PHICL in table 2).
- H-atom abstractions by H-atoms (reactions 2 to 4 in Table 2), by Cl-atoms and by phenyl radicals. H-atom abstractions lead to phenyl and chlorophenyl radicals (C₆H₄Cl, RxPHICL (x=2, 3, 4)). The rate constants of the abstractions by Cl-atom and phenyl radical were taken equal to those with H-atoms.
- Cl-atom abstractions by H-atoms (reaction 5),
- Ipso-additions of H- and Cl-atoms (reactions 6 to 9) leading to the formation of benzene (C₆H₆) and dichlorobenzene (C₆H₄Cl₂, PHI1xCL₂ (x= 2, 3, 4)), even if no trace of dichlorobenzene was identified. Ipso-additions are important due to the aromatic reactant structure.
- A molecular reaction (reaction 10) to better account for the reactant consumption in the presence of hydrogen. In our case, adding this molecular reaction had no effect on modeling results.
- Ipso-additions of phenyl radical leading to ortho, meta and para-chlorobiphenyl (o/m/p C₁₂H₉Cl) or biphenyl:



- Ipso-addition of $\text{C}_6\text{H}_4\text{Cl}$ radicals giving ortho, meta and para-chlorobiphenyl or dichlorobiphenyls ($\text{C}_{12}\text{H}_8\text{Cl}_2$):



- Terminations yielding chlorobiphenyl and dichlorobiphenyl isomers.

Due to the large number of involved heavy atoms, the rate constants of the three last types of reactions have been estimated. For ipso-additions, the rate parameters have been taken equal to those of ipso-addition of phenyl radical on benzene [17] taking into account the number of abstractable atoms. The rate parameters of terminations have been taken equal to those of the termination of two phenyl radicals yielding biphenyl [18].

To model results in presence of methane, the ipso-addition of methyl radical to chlorobenzene was added:



Its rate constant was taken equal to that of the ipso-addition of methyl radical to benzene.

For the calculation of the molecular properties of the species, the Gaussian 09 program [19] was used. Density Functional theory (DFT) at B3LYP/6-311-G(d,p) level was applied for the determination of molecular properties of reactants, intermediates and products as well as transition state structures involved in the system and not available in the literature. DFT may be one of the few applicable calculation methods for large molecule systems at the lowest computational costs and previous studies [20] [21] have shown good agreement with ab initio methods. Vibration, translation, and external rotation frequencies, moments of inertia, symmetry, spin degeneracy, and optical isomers were used for the contributions to S and Cp. Torsion frequencies were used for hindered internal rotors when present. Frequencies were identified with GaussView code.

The computer code, SMCPS [22], was used to calculate entropies S°_{298} and heat capacities $Cp^{f}_{298(T)}$ using the harmonic-oscillator approximation for vibrations, on the basis of frequencies and moments of inertia of the optimized structures. If present, torsional frequencies were not included in the contributions to entropy and heat capacities; instead, they were replaced with values from a separate analysis on each internal rotor analysis. Calculated enthalpies, entropies, heat capacities as well as optimized geometries for species and transition state structures are reported in SM. Other missing thermochemical data were taken from the database of Goos et al. [23].

4. Results and discussion

This part presents the main results obtained during the pyrolysis of neat chlorobenzene in both reactors. The effect of two hydrogen donors, H_2 and CH_4 , is also investigated in JSR.

4.1 Chlorobenzene conversion

Fig. 1 presents experimental and simulated evolution with temperature of chlorobenzene conversion obtained in JSR and TR under the same operating conditions.

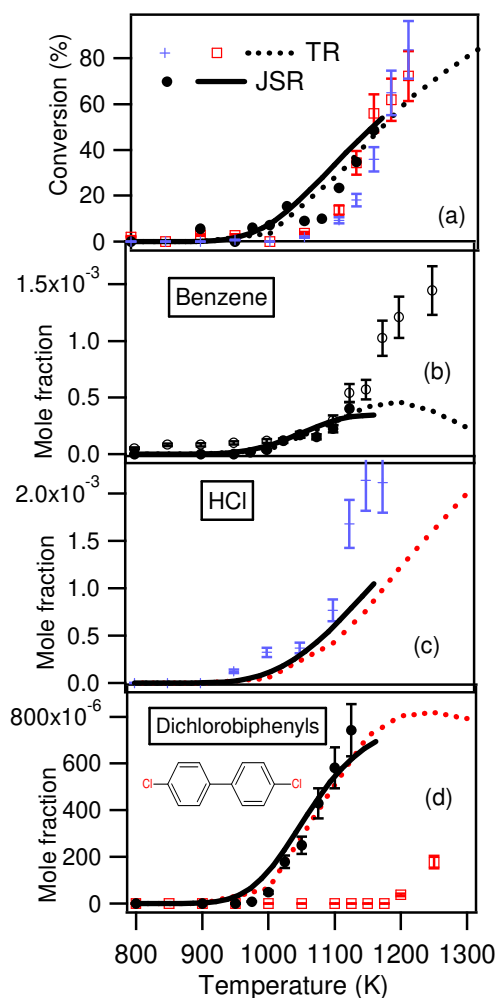


Figure 1: Evolution with temperature of (a) chlorobenzene conversion, (b) benzene, (c) HCl and (d) dichlorobiphenyls mole fractions in tubular and jet-stirred reactor (Symbols are experiments (black points and red open squares are GC measurements, blues cross are FTIR ones) and lines simulations, 0.5% chlorobenzene inlet mole fraction, $\tau = 2$ s, $P = 106.7$ kPa).

A fused silica JSR can reach a maximum possible temperature of about 1200 K. This was not high enough to fully destroy chlorobenzene. That is why the chlorobenzene pyrolysis was also studied in the alumina TR which can be used at temperatures above 1200 K.

Figure 1 shows that the type of reactor has almost no influence on chlorobenzene conversion. The molecule starts to be consumed at 900 K in both reactors. The maximum conversion in JSR (48.4%) was obtained at 1150 K, the highest studied temperature. Chlorobenzene was nearly fully destroyed in the TR (95% of conversion) at 1250 K. This was the maximum temperature where measurements were

possible with chlorobenzene/helium mixtures due to a too large pressure increase at higher temperatures preventing performing reliable experiments despite the large helium dilution. The model predicts well chlorobenzene conversion in both reactors.

Under approximately the same operating conditions using also a TR, Ritter and Bozzelli [10] obtained up to 60% of decomposition of chlorobenzene at 1228 K (residence time around 2s) in helium. The yield of chlorobenzene decomposition at 1273 K (residence time of 1.2 seconds) is about 95 % according to Rouzet et al. [9]. These results are in agreement with the present measurements.

4.2 Product formation

An important fraction of chlorobenzene was converted to a carbonaceous solid deposit on the two reactors walls. This deposit has led to many analytical problems and leads to an increasing uncertainty on experimental results with increasing temperature.

It was possible to partially remove this carbonaceous solid deposit by applying an O₂ stream to the reactor at high temperature (1200 K). Experiments of Rouzet et al. [9] revealed that the yield of chlorobenzene to soot was not important below 1123 K, but raised up to 50% at 1443 K. Ritter and Bozzelli [10] working with a TR found a soot yield of 30% at 1283 K in the absence of an hydrogen donor. Several more species have been observed in very small amounts in GC and could then not be identified.

4.2.1 Major products

Fig. 1 also presents experimental and simulated mole fraction of benzene, dichlorobiphenyls and HCl. Between 800 K and 1130 K, the influence of the reactor type on the formation of benzene and of dichlorobiphenyl isomers is limited. From approximately 1130 K, the model predicts higher formation of benzene and dichlorobiphenyls in the TR than in the JSR. Benzene and HCl mole fractions are well

predicted until 1130 K, but significantly underpredicted at higher temperatures. Dichlorobiphenyl mole fractions are well predicted in JSR, but the significant decrease in TR is not modeled. The important formation of heavy chlorinated aromatic products and soot could partly explain deviations between modeling and experiments. Above 1130 K, a deviation higher than 25 % for the C-atom material balances and 19 % for the Cl-atom material balances was observed. As shown by the deposit on the reactor wall, this came from the production of not identified heavy chlorinated compounds.

4.2.2 Minor products

To better compare the minor products distribution obtained in both reactors, a selectivity diagram has been plotted in fig. 2 for a reaction temperature of 1125 K. The selectivity is calculated as below:

$$Selectivity = \frac{x_i}{\sum_i x_i} \text{ with } x_i \text{ the mole fraction of product } i \text{ during the pyrolysis of chlorobenzene.}$$

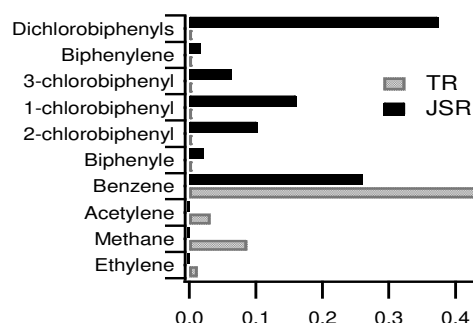


Figure 2: Carbon containing products selectivity obtained during chlorobenzene pyrolysis in both reactors (1125 K, 0.5% chlorobenzene inlet mole fraction, $\tau=2$ s, $P=106.7$ kPa).

Fig. 2 shows that more benzene, acetylene and methane are more abundant in TR than in JSR. However, the mole fraction of polychlorobiphenyls is notably reduced in TR. We assume that dichlorobiphenyls and chlorobiphenyls are secondary products and so their formation is limited in a tubular reactor. The biphenyl and biphenylene profiles are displayed in SM (figure S3 (a)), as well as methane, ethylene and acetylene profiles in JSR (figure S3 (b)).

In JSR, the model predicts well the formation of biphenyl (figure S3 (a)). The formation of biphenylene is not predicted by our model. Acetylene was not observed in JSR but very small amounts of methane and ethylene were identified (respectively 14 and 5 ppm at 1150 K).

In TR, No traces of biphenyl and biphenylene have been identified. Results of the modeling about the formation of methane, acetylene and ethylene is not shown in figure S3 (b) because their mole fraction is less than 0.6 ppm at all temperatures.

4.3 Effect of two hydrogen donors: H₂ and methane (JSR)

Cullis and Manton [24] found that the addition of hydrogen accelerated the decomposition of chlorobenzene. Louw et al. [6] postulated that using H₂ in excess would lead to a dechlorination of chlorinated aromatic compounds. Ritter and Bozzelli [25] obtained up to 99% of decomposition of chlorobenzene at 1228 K in a helium/hydrogen mixture.

Figure 3 displays the experimental and simulated JSR evolution with temperature of chlorobenzene conversion and mole fractions of benzene, toluene and dichlorobiphenyls with neat chlorobenzene and with additions of hydrogen or methane. Figure 3 shows that the experimental effect of hydrogen addition on reactant conversion is limited. However, hydrogen addition increases benzene formation and inhibits significantly the production of chlorinated polyaromatic compounds. The effect of the presence of hydrogen is well reproduced by the model.

The methane addition notably reduces chlorobenzene conversion, especially above 1000 K. This is due to the formation of toluene, a well-known radical scavenger via the formation of resonance-stabilized benzyl radicals. The formation of toluene is well predicted as shown by fig. 3c.

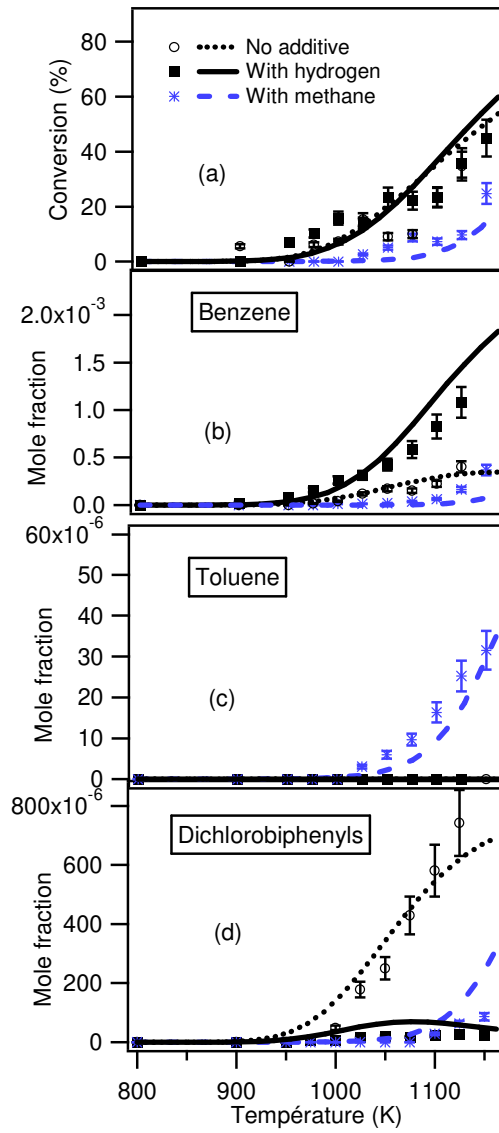


Figure 3: JSR evolution with temperature of (a) chlorobenzene conversion and mole fractions of (b) benzene, (c) toluene and (d) dichlorobiphenyls with no additive (0.5% chlorobenzene inlet mole fraction), with addition of hydrogen (0.5% chlorobenzene inlet mole fraction, 0.5% hydrogen inlet mole fraction), and with addition of methane (0.5% chlorobenzene inlet mole fraction, 0.5% methane inlet mole fraction), at $\tau = 2$ s and $P = 106.7$ kPa. Symbols are experiments (open circles for neat chlorobenzene, black squares for H_2 addition, blue stars for CH_4 addition) and lines simulations.

4.4 Discussion

As the model reproduces satisfactorily the JSR experimental results, Figure 4 presents a flow rate analysis performed at 1100 K under the conditions of Figure 3. This figure shows that, for neat chlorobenzene, the major way (33.3%) of reactant consumption is by H-abstractions yielding chlorophenyl radicals. Chlorophenyl radicals react then by ipso-addition on chlorobenzene giving isomers of dichlorobiphenyl. This is the second most important way (30.5%) of reactant consumption. The third most important way (19.0%) of reactant consumption is by Cl-abstractions producing phenyl radicals, a source of biphenyl. Minor consumption pathways (less than 10% each) include ipso-addition of H-atoms yielding benzene, ipso-addition of phenyl radicals abstracting a Cl-atom, the second source of biphenyl, and ipso-addition of phenyl radicals releasing a H-atom and producing isomers of chlorobiphenyl. Note that chlorophenyl radicals are the main source of dichlorobiphenyls. Ipso-addition of chlorophenyl radicals to benzene can also produce chlorobiphenyls.

With the addition of hydrogen, the formation of phenyl radicals and benzene is favored, while the production of dichlorobiphenyl isomers is almost completely inhibited (less of 6% of reactant consumption). In addition, chlorophenyl radicals can easily react with hydrogen to give back chlorobenzene. Consequently, in presence of hydrogen, its net rate of formation is significantly reduced. This explains why the formation of dichlorobiphenyls is notably lower as it was clearly observed in JSR experiments (by a factor of around 27 at 1100 K) and in simulations, as shown in fig. 3. Since the formation of benzene and phenyl radicals is favored, the impact of hydrogen addition on the formation of chlorobiphenyls is more limited.

Compared to neat chlorobenzene, the only difference in presence of methane is the occurrence of a new minor pathway: the production of toluene by ipso-addition of methyl radicals. Toluene is consumed by H-abstractions with H-atoms to give benzyl radicals, which can react with methane to give back toluene and with methyl radicals to produce ethylbenzene.

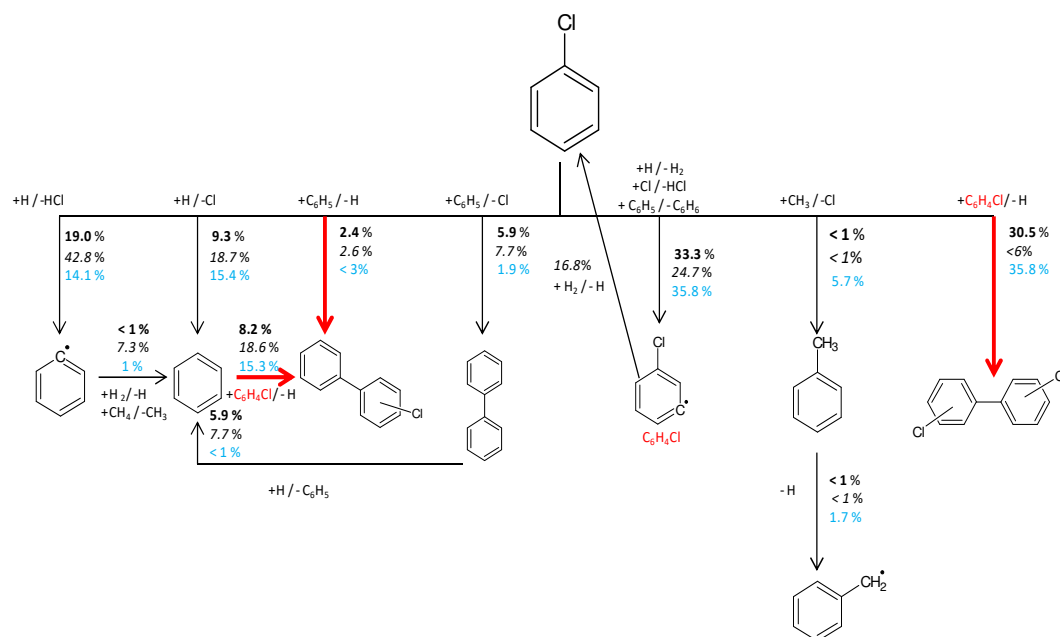


Figure 4: Flow rate analysis at 1100 K under the conditions of Figure 3. Numbers on arrows (black bold for neat chlorobenzene, black italics for H_2 addition, blue for CH_4 addition) represents the consumption rate normalized by the total chlorobenzene consumption rate. Only one isomers of chlorophenyl radical is shown for clarity; for chlorobiaromatic compounds, the chlorine atom can be carried by every atoms of the cycle. Red thick arrows correspond to the main ways of formations of chlorobiaromatic compounds.

To better understand the most influential reactions, Figure 5 presents a sensitivity analysis performed at 1100 K under the conditions of Figure 3. With neat chlorobenzene, the reactions with the largest promoting effect are the Cl-abstraction from chlorobenzene by H-atoms producing phenyl radicals, the ipso-addition of H-atom or phenyl radicals to chlorobenzene yielding benzene or biphenyl, respectively, and the unimolecular decomposition of the reactant to give phenyl radicals and chlorine atoms. The reactions of chlorophenyl radicals have also some effect. The ipso-additions to the reactant show a promoting influence, while the termination between two chlorophenyl radicals has an inhibiting effect.

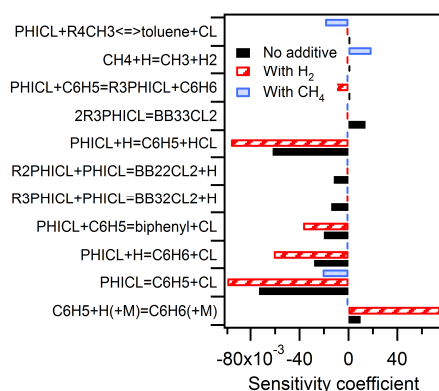


Figure 5: Sensitivity analysis on chlorobenzene mole fraction at 1100 K under the conditions of Figure 3. Reactions with a negative coefficient have a promoting effect on the reactivity.

For the H₂ addition case, the promoting effect of the four reactions displaying the largest negative sensitivity coefficient in neat chlorobenzene is still enhanced. Note also a significant increase of the inhibiting effect of the combination of phenyl radicals with H-atoms. The fact that the sensitivity coefficient of the chlorophenyl radical reactions are close to zero confirms the significant reduction of their formation pathways, as it was discussed previously together with Figure 4.

For the CH₄ addition case, the only of the four reactions displaying the largest negative sensitivity coefficient in neat chlorobenzene keeping some influence, even if reduced, is the unimolecular decomposition. This shows that the influence of all the radical reactions is significantly reduced. Additional reactions showing some influence are the ipso-addition of methyl radicals to chlorobenzene producing toluene and the H-abstraction from methane by H-atoms.

5. Conclusion

A study of chlorobenzene pyrolysis has been carried out in two different reactors: a jet-stirred reactor and a tubular reactor. Temperatures were ranging from 800 to 1125 K in the JSR and from 800 to 1250 K in the TR. Residence time was in both reactors equal to 2 s with a chlorobenzene inlet mole fraction of 0.005. All experiments were performed at a pressure of 106.7 kPa. The following products

were identified: **HCl**, H₂, Methane, ethylene, acetylene, ethane, **benzene**, biphenyl, biphenylene, chlorobiphenyls and **dichlorobiphenyls** with all of their isomers. Products written in bold are major products. An important formation of a carbonaceous solid deposit was observed in both reactors involving an increasing uncertainty on experimental results when temperature rises.

Tests for the addition of hydrogen donors (H₂ and CH₄) were made in order to limit the formation of biaromatic compounds and of carbonaceous solid. The addition of hydrogen in JSR leads to an increase of the benzene mole fraction and inhibits significantly the formation of dichlorobiphenyls. The addition of methane also inhibits the production of undesired chlorinated aromatic compounds, but it also decreases the reactant conversion due to the formation of toluene. The use of a process based on thermal decomposition to destroy PCBs can then be envisaged as an alternative solution to incineration only with a planned significant addition of hydrogen.

Since there is a lack of kinetic data in the literature about chlorinated compounds, a first approach detailed kinetic model has been developed based on theoretically calculated rate parameters. According to uncertainties in experimental results, this model gives satisfactory predictions of the reactivity and formation of major compounds, as well as the effect of the addition of hydrogen donors. However, improvements in the model are certainly needed to refine the prediction of minor products.

Acknowledgements

This work has been supported by TERBIS, 943 rue Pasteur, 60700 Pont Sainte Maxence, France.

References

- [1] [Online]. Available: <http://www.greenfacts.org/en/pcbs/1-2/1-polychlorinated-biphenyls.htm>.
- [2] V. S. Rao and G. B. Skinner, *J. Phys. Chem*, vol. 88, pp. 5990-5995, 1984.
- [3] V. S. Rao and G. B. Skinner, *J. Phys. Chem.*, vol. 92, pp. 2442-2448, 1988.
- [4] J. P. Cui, Y. Z. He and W. Tsang, *J. Phys. Chem.*, vol. 93, pp. 724-727, 1988.
- [5] R. D. Kern, K. Xie and H. Chen, *Combust. Sci. and Tech.*, vol. 85, pp. 77-86, 1992.
- [6] R. Louw, J. Rothulen and R. Wegman, *J. Phys. Chem.*, vol. 93, pp. 724-727, 1989.
- [7] R. W. Ross, F. C. Whitmore and R. A. Carnes, *Hazardous Waste* , vol. 1, pp. 581-891, 1984.
- [8] K. Ballschmiter, P. Kirschmer and W. Zoller, *Chemosphere*, vol. 15, pp. 1369-1372, 1986.
- [9] G. Rouzet, D. Schwarz, R. Gadiou and L. Delfosse, *J. Anal. Appl. Pyrolysis*, vol. 57, pp. 153-168, 2001.
- [10] E. R. Ritter, J. W. Bozzelli and A. M. Dean, *J. Phys. Chem*, vol. 94, pp. 2493-2504, 1990.
- [11] A. Cuoci, A. Frassoldati, T. Faravelli and E. Ranzi, *Comp. Phys. Com.*, vol. 192, pp. 237-264, 2015.
- [12] H. Zhang, X. Zhang, D. Truhlar and X. Xu, *J. Phys. Chem. A*, vol. 121, pp. 9033-9044, 2017.
- [13] B. Giri, T. Bentz, H. Hippler and M. Olzmann, *Zeitschrift für Physikalische Chemie*, vol. 223, pp. 539-549, 2009.
- [14] B. Husson, M. Ferrari, O. Herbinet, S. S. Ahmed and P.-A. Glaude, *Proc. Combust. Inst.*, vol. 34, pp. 325-333, 2013.
- [15] M. Pelucchi, A. Frassodalti, T. Faravelli, B. Ruscic and P. Glarborg, *Combust. Flame*, vol. 162, pp. 2693-2704, 2015.
- [16] Y. R. Luo, *Comprehensive Handbook of Chemical Bond Energies*, 2007.

- [17] H. Wang and M. Frenklach, *Combust. Flame*, vol. 110, pp. 173-221, 1997.
- [18] R. S. Tranter, S. J. Klippenstein, L. B. Harding, B. R. Giri, X. Yang and J. H. Kiefer, *J. Phys. Chem. A*, vol. 114, pp. 8240-8261, 2010.
- [19] M. J. Frisch, G. W. Trucks, H. B. Schlegel, G. E. Scuseria, M. A. Robb and J. R. Cheeseman, *Gaussian 09, Revision A02*, Wallingford CT, 2016.
- [20] N. Sebbar, J. W. Bozzelli and H. J. Bockhorn, *Phys. Chem. A*, vol. 115, pp. 11897-11914, 2011.
- [21] L. Zhu and J. W. Bozzelli, *J. Phys. Chem.*, vol. 32, p. 1713, 2003.
- [22] C. Sheng, Ph.D Dissertation. Department of Chemical Engineering. Chemistry and Environmental Science, New Jersey Institute of Technology, Newark, 2002.
- [23] E. Goos, A. Burcat and B. Ruscic, *Third Millenium Ideal Gas and Condensed Phase Thermochemical Database for Combustion with Updates from Active Thermochemical Tables*, 2005.
- [24] C. F. Cullis and J. E. Manton, *Trans. Farad. Soc.*, vol. 54, pp. 381-389, 1958.
- [25] E. Ritter and J. W. Bozzelli, *Hazardous Waste Hazardous Material*, vol. 75, p. 103, 1990.

List of figure captions

Figure 1: Evolution with temperature of (a) chlorobenzene conversion, (b) benzene, (c) HCl and (d) dichlorobiphenyls mole fractions in tubular and jet-stirred reactor (Symbols are experiments (black points and red open squares are GC measurements, blues cross are FTIR ones) and lines simulations, 0.5% chlorobenzene inlet mole fraction, $\tau = 2$ s, $P = 106.7$ kPa).

Figure 2: Carbon containing product selectivity obtained during chlorobenzene pyrolysis in both reactors (1125 K, 0.5% chlorobenzene inlet mole fraction, $\tau = 2$ s, $P = 106.7$ kPa).

Figure 3: JSR evolution with temperature of (a) chlorobenzene conversion and mole fractions of (b) benzene, (c) toluene and (d) dichlorobiphenyls with no additive (0.5% chlorobenzene inlet mole fraction), with addition of hydrogen (0.5% chlorobenzene inlet mole fraction, 0.5% hydrogen inlet mole fraction), and with addition of methane (0.5% chlorobenzene inlet mole fraction, 0.5% methane inlet mole fraction), at $\tau = 2$ s and $P = 106.7$ kPa. Symbols are experiments (open circles for neat chlorobenzene, black squares for H_2 addition, blue stars for CH_4 addition) and lines simulations.

Figure 4: Figure 4: Flow rate analysis at 1100 K under the conditions of Figure 3. Numbers on arrows (black bold for neat chlorobenzene, black italics for H_2 addition, blue for CH_4 addition) represents the consumption rate normalized by the total chlorobenzene consumption rate. Only one isomers of chlorophenyl radical is shown for clarity; for chlorobiaromatic compounds, the chlorine atom can be carried by every atoms of the cycle. Red thick arrows correspond to the main ways of formations of chlorobiaromatic compounds.

Figure 5: Sensitivity analysis on chlorobenzene mole fraction at 1100 K under the conditions of Figure 3. Reactions with a negative coefficient have a promoting effect on the reactivity.

List of tables

Table 1: Experimental inlet composition

Mixture	Neat chlorobenzene	+ H_2	+ CH_4
Composition (%)	0.5 C_6H_5Cl + 99.5 He	0.5 C_6H_5Cl + 0.5 H_2 + 99.0 He	0.5 C_6H_5Cl + 0.5 CH_4 + 99.0 He
Used reactors	JSR and TR	JSR	JSR

Table 2: Theoretically calculated rate constants (rate parameters of reaction 1 have been recalculated in the present study).

	Reaction	A factor ($cm^3 \cdot mol^{-1} \cdot s^{-1}$)	n	Ea ($cal \cdot mol^{-1}$)
1	$C_6H_5 + H = C_6H_6 + H$	5.02×10^{11}	-0.14	2749
2	$PHICl + H = R2PHICl + H_2$	1.50×10^8	1.79	12328
3	$PHICl + H = R3PHICl + H_2$	1.23×10^8	1.81	10930
4	$PHICl + H = R4PHICl + H_2$	1.35×10^8	1.81	11748
5	$PHICl + H = C_6H_5 + HCl$	1.61×10^9	1.57	10988
6	$PHICl + H = C_6H_6 + Cl$	4.26×10^7	1.772	7951
7	$PHICl + Cl = PHI12Cl_2 + H$	1.17×10^4	2.992	22576
8	$PHICl + Cl = PHI13Cl_2 + H$	8.57×10^3	3.057	21927
9	$PHICl + Cl = PHI14Cl_2 + H$	5.48×10^3	3.027	21829
10	$PHICl + H_2 = C_6H_6 + HCl$	1.36×10^6	2.18	73174

List of Supplemental Material

- Temperature profiles measured in tubular reactor
- Discussion about the plug flow reactor assumption
- A typical IRTF spectrum obtained during the chlorobenzene pyrolysis
- Calculated enthalpies, entropies, heat capacities as well as optimized geometries for species and transition state structures
- Evolution with temperature of (a) biphenyl and biphenylene in JSR, (b) methane, ethylene, acetylene in TR, (c) methane and ethylene in JSR mole fractions (Symbols are experiments and lines simulations, 0.5% chlorobenzene inlet mole fraction, $\tau = 2$ s, $P = 106.7$ kPa).